

# Radome Enclosed Circularly Polarized Antenna System with Enhanced Beamwidth

Suman PRADHAN, Bhaskar GUPTA

Dept. of ETCE, Jadavpur University, Kolkata, India

sumanpradhan.kut2@gmail.com, gupta\_bh@yahoo.com

Submitted October 2, 2021 / Accepted December 20, 2021

**Abstract.** *This paper presents a circularly polarized (CP) patch antenna system enclosed by a nosecone radome which has a wide beam response. A U-slot loaded corner truncated patch antenna is mounted upon a conical ground structure for achieving the wide beam response. When two such antennas, one Right Handed CP (RHCP) and another Left Handed CP (LHCP) are placed inside a nosecone radome, a drastic reduction in the antenna beamwidth is observed. Finally a metallic conical ring is added to the structure which improves the beamwidth of the antenna and we achieve a beamwidth of  $74^\circ$  and  $120^\circ$  in the  $\phi=0^\circ$  and  $\phi=90^\circ$  planes respectively. The antenna system also provides a good axial ratio bandwidth performance.*

## Keywords

Beamwidth enhancement, circular polarization, conical ground, nosecone radome, U-slot loaded corner truncated microstrip patch antenna

## 1. Introduction

The function of protecting the antennas, especially those which are to be employed outdoors lies with the radome. Although the shape of the radome is determined by the application area, sometimes there may be a flexibility of selecting the shape of the radome. In many ground based antenna systems the radome may be of flat shape. The effect of placing a flat dielectric radome on antenna performance has been reported in [1]. Mainly the effect of radome on the shift in resonant frequency was reported for rectangular [2] and circular [3] patches when a dielectric superstrate was placed directly upon the patch antenna. Later it was found that placing the dielectric superstrate at some distance above the patch antenna could lead to improvement in the gain of the antenna. This phenomenon was used in [4] where a gain improvement of 7 dB was reported. In another work [5] a dielectric superstrate placed above single and array antennas resulted in 2 dB improvement in gain.

The emergence of metamaterials has made feasible

another other way of gain enhancement by flat radomes. Multiple Jerusalem crosses placed over a square patch antenna led to 3.4 dB gain improvement in [6]. A U-slot loaded patch antenna loaded with PRS along with a FSS radome led to a gain of 21 dBi in [7]. Metamaterial radomes can also be used for generating CP radiation [8] and also for gain enhancement of CP antennas. A cross S shaped metamaterial layer placed over a CP antenna led to 3.15 dB gain improvement in [9]. An SRR based metamaterial radome placed over a notch loaded circular patch antenna led to 1 dB gain improvement in [10].

In some applications like ground based radar systems the radome shape can be hemispherical. But for airborne applications the radome shape has to be streamlined like conical or tangent-ogive. These kinds of radome shapes can bring about a host of problems like boresight error (BSE), insertion loss, depolarization etc. [11]. Some of these effects can be mitigated by varying the radome thickness. The thickness of the wall can be varied in a discreet manner [12] or it can be varied continuously [13]. Generally either optimization techniques are employed to find the optimum thickness of the radome [14] or they can be based on half-wave thickness [15]. Another way of improving the radome performance is keeping the thickness of the radome wall constant and varying the dielectric constant and loss tangent of the wall in a continuous manner [16]. The performance of the antenna radome system can be further improved by multilayer radome configurations. Depending upon the arrangement of different layers they can be classified as A sandwich [17], B sandwich [18] having three layers and C sandwich [19] radome which has five layers. A seven layer radome has also been proposed in literature for superior performance [20].

Most of the solutions presented above deal with parameters like BSE and transmission coefficient but do not talk about the effect of radome on the half power beamwidth (HPBW) and axial ratio beamwidth (ARBW) in case of CP antennas. In [21] the variation of ARBW was studied for various radome materials, radome shapes and radome heights and an optimized shape was chosen. But for airborne applications the shape of the radome has to be streamlined which means the radome has to be of conical shape. In this paper we study the effect of placing a conical

radome on the performance of a CP antenna and provide a solution for recovering the CP antenna performance. The solutions for performance enhancement of radome enclosed antennas are either variable thickness radomes or multilayer radomes. It is very difficult to fabricate the variable thickness radomes and errors may come in the thickness profile. The multilayer radomes are costly to fabricate. We provide a cost effective solution which is easier to fabricate.

As depolarization is a common phenomenon found in radome enclosed antennas we choose a CP antenna which has large ARBW. The antennas which provide a high ARBW often require a shaped ground plane [22], [23]. We select the one reported in [24] because the antenna has the highest ARBW. The first section deals with the CP antenna design and extensive parametric studies are carried out. Next the antenna is placed inside a conical radome and the antenna performance is studied. It is observed that the antenna beamwidth is drastically reduced due to the presence of conical radome. Next a metallic conical ring is placed inside the radome which leads to beamwidth improvement of the radome enclosed antenna. Finally the efficacy of the solution is validated by measured results.

## 2. U-Slot Loaded Corner Truncated Patch Antenna Located upon Conical Ground

A U-slot loaded corner truncated patch antenna which produces a wideband CP response when placed upon a conical ground plane can simultaneously give rise to a wide beamwidth pattern [24]. The antenna structure is shown in Fig. 1.

The design frequency is chosen to be 9 GHz. The substrate taken is ARLON AD 250 with dielectric constant ( $\epsilon_r$ ) of 2.5, thickness of 1.524 mm with a loss tangent ( $\tan\delta$ ) of 0.0018. Simulating only the U-slot loaded corner truncated patch antenna using CST Studio Suite [25], the dimensions of the antenna for obtaining the minimum axial ratio in dB at 9 GHz is found out. The dimensions are  $a = 9.4$  mm,  $i = 1.9$  mm,  $d = 4.2$  mm,  $L_x = 3.2$  mm,  $L_y = 2.6$  mm,  $g = 0.4$  mm,  $u = 3.9$  mm and  $s = 11.4$  mm.

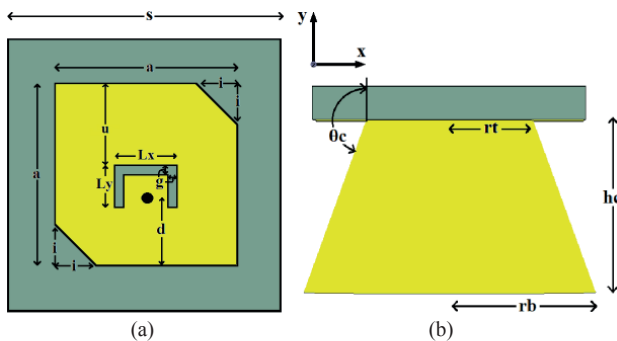


Fig. 1. (a) U-slot loaded corner truncated patch antenna and (b) patch antenna placed upon a conical ground plane.

The metallic cone which is to be placed beneath the patch antenna has a height  $h_c$  and angle  $\theta_c$  with a top and bottom radius of  $r_t$  and  $r_b$ , respectively. To study the effect of metal cone on the antenna performance the parameters  $r_t$ ,  $h_c$  and  $\theta_c$  are varied.

It can be observed that for  $\theta_c$  values of  $130^\circ$  and  $145^\circ$ , there is an increase in the ARBD when  $r_t$  is increased.

rt (mm)	$\theta_c = 130^\circ$		$\theta_c = 145^\circ$		$\theta_c = 160^\circ$	
	ARBD (MHz)	Gain (dBi)	ARBD (MHz)	Gain (dBi)	ARBD (MHz)	Gain (dBi)
4	8947-9148 (201)	5.073	8919-9132 (213)	5.537	8891-9112 (221)	5.940
5	8943-9146 (203)	5.433	8923-9137 (214)	5.605	8900-9121 (221)	5.866
6	8946-9151 (205)	5.703	8931-9146 (215)	5.738	8916-9135 (219)	5.898

Tab. 1. Axial Ratio Bandwidth (ARBD) and gain variation for different  $r_t$  and  $\theta_c$  when  $h_c = 6$  mm.

rt (mm)	$\theta_c = 130^\circ$		$\theta_c = 145^\circ$		$\theta_c = 160^\circ$	
	ARBD (MHz)	Gain (dBi)	ARBD (MHz)	Gain (dBi)	ARBD (MHz)	Gain (dBi)
4	8958-9119 (161)	3.526	8938-9118 (180)	3.745	8903-9117 (214)	5.137
5	8946-9128 (182)	4.290	8937-9125 (188)	4.221	8914-9123 (209)	4.995
6	8944-9139 (195)	4.821	8940-9136 (196)	4.680	8927-9135 (208)	5.056

Tab. 2. Axial Ratio Bandwidth (ARBD) and gain variation for different  $r_t$  and  $\theta_c$  when  $h_c = 8$  mm.

rt (mm)	$\theta_c = 130^\circ$		$\theta_c = 145^\circ$		$\theta_c = 160^\circ$	
	ARBD (MHz)	Gain (dBi)	ARBD (MHz)	Gain (dBi)	ARBD (MHz)	Gain (dBi)
4	8913-9084 (171)	3.297	8897-9058 (161)	3.745	8886-9079 (193)	4.016
5	8909-9091 (182)	3.922	8887-9075 (188)	4.221	8886-9077 (191)	4.017
6	8906-9104 (198)	4.412	8900-9094 (194)	4.680	8897-9091 (194)	4.281

Tab. 3. Axial Ratio Bandwidth (ARBD) and gain variation for different  $r_t$  and  $\theta_c$  when  $h_c = 10$  mm.

rt (mm)	$\theta_c = 130^\circ$		$\theta_c = 145^\circ$		$\theta_c = 160^\circ$	
	ARBD (MHz)	Gain (dBi)	ARBD (MHz)	Gain (dBi)	ARBD (MHz)	Gain (dBi)
4	8890-9080 (190)	3.760	8859-9047 (188)	4.505	8855-9046 (191)	4.682
5	8886-9086 (200)	4.173	8937-9125 (188)	4.221	8860-9050 (190)	4.365
6	8897-9099 (202)	4.685	8940-9136 (196)	4.680	8876-9073 (197)	4.554

Tab. 4. Axial Ratio Bandwidth (ARBD) and gain variation for different  $r_t$  and  $\theta_c$  when  $h_c = 12$  mm.

When  $\theta_c$  is  $160^\circ$  the ARBD decreases with increasing  $rt$  for both  $hc = 6$  mm and  $hc = 8$  mm, whereas for  $hc = 10$  mm and  $hc = 12$  mm the ARBD first decreases and then increases for increase in  $rt$ .

Next we study both the HPBW and ARBW of the antenna for the same ground cone variations as before. We define the angles which fall both within HPBW and ARBW as the usable bandwidth (USBW) of the antenna. Our objective will be to maximize the USBW of the antenna.

When the height is 6 mm the USBW is around  $100^\circ$ . When  $hc = 8$  mm the ARBW increases with increase in  $\theta_c$ . But the HPBW decreases for  $rt = 4$  mm and  $rt = 5$  mm

rt (mm)	$\theta_c = 130^\circ$		$\theta_c = 145^\circ$		$\theta_c = 160^\circ$	
	$\phi=0^\circ$	$\phi=90^\circ$	$\phi=0^\circ$	$\phi=90^\circ$	$\phi=0^\circ$	$\phi=90^\circ$
4	H: $-47^\circ$ to $48^\circ$ (95°)	H: $-56^\circ$ to $39^\circ$ (95°)	H: $-41^\circ$ to $44^\circ$ (85°)	H: $-47^\circ$ to $39^\circ$ (86°)	H: $-47^\circ$ to $49^\circ$ (96°)	H: $-52^\circ$ to $46^\circ$ (98°)
	A: $-69^\circ$ to $45^\circ$ (114°)	A: $-51^\circ$ to $51^\circ$ (102°)	A: $-96^\circ$ to $61^\circ$ (157°)	A: $-71^\circ$ to $63^\circ$ (134°)	A: $-82^\circ$ to $79^\circ$ (161°)	A: $-92^\circ$ to $73^\circ$ (165°)
	U: $92^\circ$	U: $90^\circ$	U: $85^\circ$	U: $86^\circ$	U: $96^\circ$	U: $98^\circ$
5	H: $-56^\circ$ to $53^\circ$ (109°)	H: $-63^\circ$ to $45^\circ$ (108°)	H: $-52^\circ$ to $52^\circ$ (104°)	H: $-59^\circ$ to $47^\circ$ (106°)	H: $-49^\circ$ to $49^\circ$ (98°)	H: $-55^\circ$ to $46^\circ$ (101°)
	A: $-60^\circ$ to $43^\circ$ (103°)	A: $-50^\circ$ to $56^\circ$ (106°)	A: $-100^\circ$ to $55^\circ$ (155°)	A: $-59^\circ$ to $60^\circ$ (119°)	A: $-90^\circ$ to $67^\circ$ (157°)	A: $-79^\circ$ to $67^\circ$ (146°)
	U: $99^\circ$	U: $95^\circ$	U: $104^\circ$	U: $106^\circ$	U: $98^\circ$	U: $101^\circ$
6	H: $-55^\circ$ to $49^\circ$ (104°)	H: $-60^\circ$ to $43^\circ$ (103°)	H: $-53^\circ$ to $50^\circ$ (103°)	H: $-59^\circ$ to $45^\circ$ (104°)	H: $-50^\circ$ to $49^\circ$ (99°)	H: $-56^\circ$ to $45^\circ$ (101°)
	A: $-56^\circ$ to $45^\circ$ (101°)	A: $-46^\circ$ to $61^\circ$ (107°)	A: $-96^\circ$ to $52^\circ$ (148°)	A: $-53^\circ$ to $62^\circ$ (115°)	A: $-97^\circ$ to $58^\circ$ (155°)	A: $-66^\circ$ to $67^\circ$ (133°)
	U: $100^\circ$	U: $89^\circ$	U: $103^\circ$	U: $98^\circ$	U: $99^\circ$	U: $101^\circ$

Tab. 5. Variation of HPBW (H), ARBW (A) and USBW (U) for different  $rt$  and  $\theta_c$  when  $hc = 6$  mm.

rt (mm)	$\theta_c = 130^\circ$		$\theta_c = 145^\circ$		$\theta_c = 160^\circ$	
	$\phi=0^\circ$	$\phi=90^\circ$	$\phi=0^\circ$	$\phi=90^\circ$	$\phi=0^\circ$	$\phi=90^\circ$
4	H: $-74^\circ$ to $82^\circ$ (156°)	H: $-88^\circ$ to $63^\circ$ (151°)	H: $-69^\circ$ to $77^\circ$ (146°)	H: $-81^\circ$ to $66^\circ$ (147°)	H: $-53^\circ$ to $55^\circ$ (108°)	H: $-58^\circ$ to $54^\circ$ (112°)
	A: $-36^\circ$ to $26^\circ$ (62°)	A: $-48^\circ$ to $52^\circ$ (100°)	A: $-51^\circ$ to $44^\circ$ (95°)	A: $-58^\circ$ to $59^\circ$ (117°)	A: $-94^\circ$ to $76^\circ$ (170°)	A: $-90^\circ$ to $76^\circ$ (166°)
	U: $62^\circ$	U: $100^\circ$	U: $95^\circ$	U: $117^\circ$	U: $108^\circ$	U: $112^\circ$
5	H: $-68^\circ$ to $68^\circ$ (136°)	H: $-77^\circ$ to $53^\circ$ (130°)	H: $-66^\circ$ to $69^\circ$ (135°)	H: $-77^\circ$ to $58^\circ$ (135°)	H: $-56^\circ$ to $58^\circ$ (114°)	H: $-64^\circ$ to $54^\circ$ (118°)
	A: $-39^\circ$ to $34^\circ$ (73°)	A: $-47^\circ$ to $56^\circ$ (103°)	A: $-50^\circ$ to $44^\circ$ (94°)	A: $-54^\circ$ to $60^\circ$ (114°)	A: $-97^\circ$ to $62^\circ$ (159°)	A: $-67^\circ$ to $67^\circ$ (134°)
	U: $73^\circ$	U: $100^\circ$	U: $94^\circ$	U: $112^\circ$	U: $114^\circ$	U: $118^\circ$
6	H: $-63^\circ$ to $60^\circ$ (123°)	H: $-70^\circ$ to $48^\circ$ (118°)	H: $-63^\circ$ to $61^\circ$ (124°)	H: $-72^\circ$ to $52^\circ$ (124°)	H: $-57^\circ$ to $56^\circ$ (113°)	H: $-65^\circ$ to $52^\circ$ (117°)
	A: $-44^\circ$ to $38^\circ$ (82°)	A: $-47^\circ$ to $65^\circ$ (112°)	A: $-50^\circ$ to $48^\circ$ (98°)	A: $-50^\circ$ to $64^\circ$ (114°)	A: $-84^\circ$ to $57^\circ$ (141°)	A: $-59^\circ$ to $66^\circ$ (125°)
	U: $82^\circ$	U: $95^\circ$	U: $98^\circ$	U: $102^\circ$	U: $113^\circ$	U: $111^\circ$

Tab. 6. Variation of HPBW (H), ARBW (A) and USBW (U) for different  $rt$  and  $\theta_c$  when  $hc = 8$  mm.

rt (mm)	$\theta_c = 130^\circ$		$\theta_c = 145^\circ$		$\theta_c = 160^\circ$	
	$\phi=0^\circ$	$\phi=90^\circ$	$\phi=0^\circ$	$\phi=90^\circ$	$\phi=0^\circ$	$\phi=90^\circ$
4	H: $-77^\circ$ to $82^\circ$ (159°)	H: $-97^\circ$ to $66^\circ$ (163°)	H: $-78^\circ$ to $90^\circ$ (168°)	H: $-97^\circ$ to $75^\circ$ (172°)	H: $-63^\circ$ to $65^\circ$ (128°)	H: $-72^\circ$ to $66^\circ$ (138°)
	A: $-42^\circ$ to $26^\circ$ (68°)	A: $-44^\circ$ to $64^\circ$ (108°)	A: $-36^\circ$ to $34^\circ$ (70°)	A: $-52^\circ$ to $61^\circ$ (113°)	A: $-94^\circ$ to $65^\circ$ (159°)	A: $-69^\circ$ to $75^\circ$ (144°)
	U: $68^\circ$	U: $108^\circ$	U: $70^\circ$	U: $113^\circ$	U: $128^\circ$	U: $135^\circ$
5	H: $-69^\circ$ to $70^\circ$ (139°)	H: $-85^\circ$ to $59^\circ$ (144°)	H: $-75^\circ$ to $78^\circ$ (153°)	H: $-94^\circ$ to $67^\circ$ (161°)	H: $-66^\circ$ to $69^\circ$ (135°)	H: $-80^\circ$ to $65^\circ$ (145°)
	A: $-50^\circ$ to $39^\circ$ (89°)	A: $-43^\circ$ to $68^\circ$ (111°)	A: $-46^\circ$ to $45^\circ$ (91°)	A: $-48^\circ$ to $65^\circ$ (113°)	A: $-63^\circ$ to $59^\circ$ (122°)	A: $-57^\circ$ to $67^\circ$ (124°)
	U: $89^\circ$	U: $102^\circ$	U: $91^\circ$	U: $113^\circ$	U: $122^\circ$	U: $122^\circ$
6	H: $-65^\circ$ to $63^\circ$ (128°)	H: $-78^\circ$ to $55^\circ$ (133°)	H: $-67^\circ$ to $65^\circ$ (132°)	H: $-83^\circ$ to $57^\circ$ (140°)	H: $-65^\circ$ to $64^\circ$ (129°)	H: $-79^\circ$ to $60^\circ$ (139°)
	A: $-54^\circ$ to $47^\circ$ (101°)	A: $-42^\circ$ to $75^\circ$ (117°)	A: $-52^\circ$ to $51^\circ$ (103°)	A: $-47^\circ$ to $70^\circ$ (117°)	A: $-61^\circ$ to $57^\circ$ (118°)	A: $-52^\circ$ to $68^\circ$ (120°)
	U: $101^\circ$	U: $97^\circ$	U: $103^\circ$	U: $104^\circ$	U: $118^\circ$	U: $112^\circ$

Tab. 7. Variation of HPBW (H), ARBW (A) and USBW (U) for different  $rt$  and  $\theta_c$  when  $hc = 10$  mm.

rt (mm)	$\theta_c = 130^\circ$		$\theta_c = 145^\circ$		$\theta_c = 160^\circ$	
	$\phi=0^\circ$	$\phi=90^\circ$	$\phi=0^\circ$	$\phi=90^\circ$	$\phi=0^\circ$	$\phi=90^\circ$
4	H: $-69^\circ$ to $74^\circ$ (143°)	H: $-90^\circ$ to $62^\circ$ (152°)	H: $-44^\circ$ to $52^\circ$ (96°)	H: $-73^\circ$ to $49^\circ$ (122°)	H: $-49^\circ$ to $43^\circ$ (92°)	H: $-72^\circ$ to $66^\circ$ (138°)
	A: $-47^\circ$ to $36^\circ$ (83°)	A: $-42^\circ$ to $70^\circ$ (112°)	A: $-45^\circ$ to $44^\circ$ (89°)	A: $-46^\circ$ to $56^\circ$ (102°)	A: $-49^\circ$ to $57^\circ$ (106°)	A: $-49^\circ$ to $51^\circ$ (100°)
	U: $83^\circ$	U: $104^\circ$	U: $88^\circ$	U: $95^\circ$	U: $92^\circ$	U: $100^\circ$
5	H: $-65^\circ$ to $67^\circ$ (132°)	H: $-83^\circ$ to $58^\circ$ (141°)	H: $-55^\circ$ to $61^\circ$ (116°)	H: $-84^\circ$ to $53^\circ$ (137°)	H: $-56^\circ$ to $54^\circ$ (110°)	H: $-76^\circ$ to $57^\circ$ (133°)
	A: $-53^\circ$ to $48^\circ$ (101°)	A: $-43^\circ$ to $76^\circ$ (119°)	A: $-49^\circ$ to $51^\circ$ (100°)	A: $-48^\circ$ to $66^\circ$ (114°)	A: $-50^\circ$ to $56^\circ$ (106°)	A: $-55^\circ$ to $63^\circ$ (118°)
	U: $101^\circ$	U: $101^\circ$	U: $100^\circ$	U: $101^\circ$	U: $104^\circ$	U: $112^\circ$
6	H: $-62^\circ$ to $61^\circ$ (123°)	H: $-78^\circ$ to $55^\circ$ (133°)	H: $-55^\circ$ to $56^\circ$ (111°)	H: $-76^\circ$ to $50^\circ$ (126°)	H: $-54^\circ$ to $54^\circ$ (108°)	H: $-76^\circ$ to $54^\circ$ (130°)
	A: $-54^\circ$ to $56^\circ$ (110°)	A: $-76^\circ$ to $54^\circ$ (130°)	A: $-54^\circ$ to $57^\circ$ (111°)	A: $-48^\circ$ to $73^\circ$ (121°)	A: $-53^\circ$ to $60^\circ$ (113°)	A: $-52^\circ$ to $68^\circ$ (120°)
	U: $110^\circ$	U: $130^\circ$	U: $110^\circ$	U: $98^\circ$	U: $107^\circ$	U: $106^\circ$

Tab. 8. Variation of HPBW (H), ARBW (A) and USBW (U) for different  $rt$  and  $\theta_c$  when  $hc = 12$  mm.

whereas for  $rt = 6$  mm the HPBW first increases and then decreases with increase in  $\theta_c$ . When  $hc = 10$  mm for all cases of  $rt$  the HPBW increases and then decreases whereas the ARBW increases with increases with  $\theta_c$ . When  $hc = 12$  mm, the HPBW is highest when  $\theta_c = 130^\circ$  for every value of  $rt$ . For  $rt = 4$  mm &  $rt = 5$  mm the ARBW is highest for  $\theta_c = 160^\circ$  but for  $rt = 6$  mm the ARBW is maximum for  $\theta_c = 130^\circ$ .

If we consider the USBW for  $hc = 8$  mm, it increases with increase in  $\theta_c$  and we get the best USBW when  $rt = 5$  mm. When  $hc = 10$  mm the USBW increases with increase in  $\theta_c$  and the best values are obtained for  $rt = 4$  mm. When  $hc = 12$  mm the best value of USBW is obtained for

$rt = 6 \text{ mm}$  and  $\theta_c = 130^\circ$ . But the USBW for  $hc = 12 \text{ mm}$  is inferior to that obtained for  $hc = 10 \text{ mm}$ . Therefore increasing  $hc$  to  $12 \text{ mm}$  does not make sense. In the next section we observe the effect of placing the antenna inside a conical radome.

### 3. Two Antenna System Enclosed in Nosecone Radome

Many transceiver systems require two antennas with opposite polarizations to maintain diversity between the transmitted and received signals. This may be the case for airborne vehicles maintaining a communication link with ground station. Therefore we take two antennas, one RHCP and another LHCP, placed side by side, both of them placed upon a conical ground. Figure 2 shows the nosecone radome made of Teflon material inside which the two antenna system is going to be placed.

The dimensions of the radome are  $D_b = 38 \text{ mm}$ ,  $D_m = 10.36 \text{ mm}$ ,  $D_t = 9.97 \text{ mm}$ ,  $t = 1.5 \text{ mm}$ ,  $h_1 = 6.8 \text{ mm}$ ,  $h_2 = 55.4 \text{ mm}$  and  $\psi = 76^\circ$ . The dimensions of the RHCP and LHCP antenna are  $a = 9.4 \text{ mm}$ ,  $i = 1.9 \text{ mm}$ ,  $d = 4.2 \text{ mm}$ ,  $L_x = 3.2 \text{ mm}$ ,  $L_y = 2.6 \text{ mm}$ ,  $g = 0.4 \text{ mm}$ ,  $u = 3.9 \text{ mm}$  and  $s = 11.4 \text{ mm}$  and the dimension of the conical ground is  $rt = 5 \text{ mm}$ ,  $\theta_c = 160^\circ$  and  $hc = 8 \text{ mm}$ . Figure 3 shows the arrangement of the two antennas which are placed on a Teflon base of diameter  $D_b + 2t$ . The antennas are placed at a gap  $p$  which is taken as  $2rb$ .

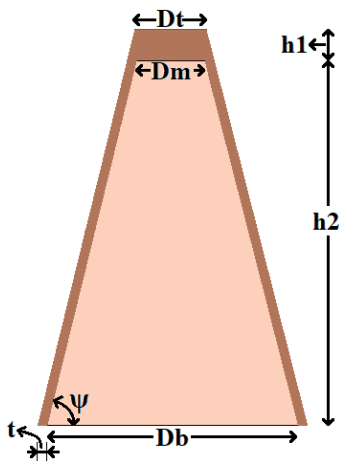


Fig. 2. Side view of nosecone radome made of Teflon.

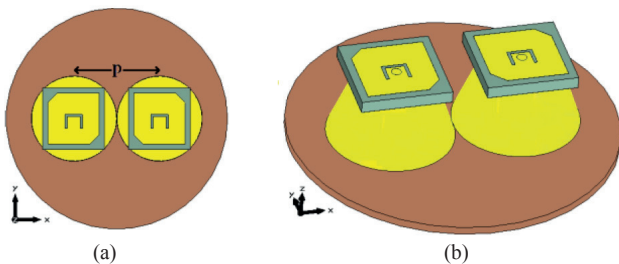


Fig. 3. Two antenna system placed upon a Teflon base: (a) top view and (b) lateral view.

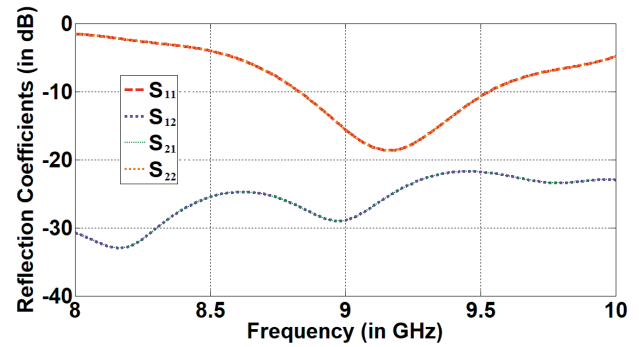


Fig. 4. Reflection coefficients of the antenna system.

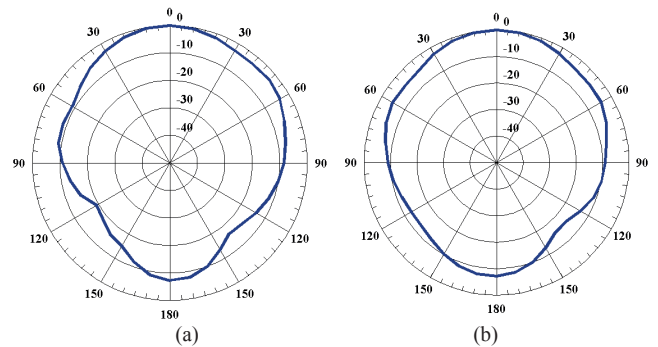


Fig. 5. Normalized radiation pattern of the RHCP antenna in (a)  $\phi = 0^\circ$  and (b)  $\phi = 90^\circ$  plane.

PARAMETER	VALUE
AR bandwidth (GHz)	9.162–9.360 (2.14%)
AR beamwidth ( $\phi = 0^\circ$ )	$-54^\circ$ – $47^\circ$ ( $101^\circ$ )
AR beamwidth ( $\phi = 90^\circ$ )	$-60^\circ$ – $60^\circ$ ( $120^\circ$ )
HPBW ( $\phi = 0^\circ$ )	$-29^\circ$ – $33^\circ$ ( $62^\circ$ )
HPBW ( $\phi = 90^\circ$ )	$-31^\circ$ – $32^\circ$ ( $63^\circ$ )
Usable beamwidth ( $\phi = 0^\circ$ )	$-29^\circ$ – $33^\circ$ ( $62^\circ$ )
Usable beamwidth ( $\phi = 90^\circ$ )	$-31^\circ$ – $32^\circ$ ( $63^\circ$ )
Impedance bandwidth (GHz)	8.814–9.673 (9.29%)
Gain (dBi)	6.9

Tab. 9. Various parameters of the radome enclosed two antenna system.

The reflection coefficients of the antenna system are shown in Fig. 4. As expected the performance of the RHCP and LHCP antenna are identical. The isolation between the two antennas is in excess of 20 dB.

The radiation pattern of the RHCP antenna in both the principal planes is shown in Fig. 5. The performance of the radome enclosed two antenna system is summarized in Tab. 9.

Comparing the performance of the antenna inside radome with the patch antenna without the radome whose performance was tabulated in Tab. 6, we find that the HPBW has degraded from  $114^\circ$  and  $118^\circ$  to  $62^\circ$  and  $63^\circ$  for the  $\phi = 0^\circ$  and  $\phi = 90^\circ$  planes respectively. Similarly the ARBW has degraded from  $159^\circ$  and  $134^\circ$  to  $101^\circ$  and  $120^\circ$  for the  $\phi = 0^\circ$  and  $\phi = 90^\circ$  planes respectively. Therefore the USBW has also degraded from  $114^\circ$  and  $118^\circ$  to  $62^\circ$  and  $63^\circ$  for the  $\phi = 0^\circ$  and  $\phi = 90^\circ$  planes respectively. These results clearly show the effect of the nosecone radome in degradation of the beamwidth of the antenna.

The decrease in all the beamwidths certainly gives rise to the increase in the gain of the antenna.

### 4. Radome Enclosed Two Antenna System with Metallic Conical Ring

From the previous section we observed that the nosecone radome will make the radiation pattern narrow. This happens due to the multiple reflection and refraction of the radiated field from the radome wall. To have more radiation towards the off broadside direction we place a metallic structure in the broadside radiation so that it reflects some of the radiated fields and scatters it to off boresight directions. We use a metallic conical ring whose dimension is chosen in such a way that it fits inside the top of the radome. The metallic conical structure is shown in Fig. 6. The final arrangement of the two antennas inside the nosecone radome with the metallic ring on top is shown in Fig. 7.

To study the effect of the metallic ring on the antenna performance we perform extensive parametric studies. The top radius of the conical ground (rt) is fixed at 5 mm. The angle of the conical ground cannot be varied by a large extent due to the limited space available inside the radome. When the thickness of the metallic ring (tr) is 2 mm and higher there is no significant improvement in the antenna performance. Therefore we fix the thickness of the metallic ring at 1 mm and vary the height of the ring.

It can be observed that there is a decline in gain with increasing hc which points to an increase in beamwidths. When hr is increased there is an increase in gain except for the case when hc = 9 mm and  $\theta_c = 165^\circ$ . The ARBD declines when we increase hc. Next we study both the HPBW and ARBW of the antenna for various hc and  $\theta_c$  variations for different values of hr.

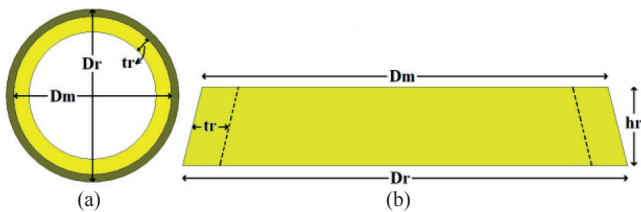


Fig. 6. Metallic conical ring: (a) top view and (b) side view.

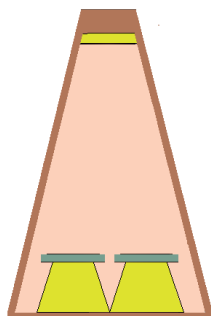


Fig. 7. Final antenna assembly.

hc (mm)	$\theta_c = 155^\circ$		$\theta_c = 160^\circ$		$\theta_c = 165^\circ$	
	ARBD (MHz)	Gain (dBi)	ARBD (MHz)	Gain (dBi)	ARBD (MHz)	Gain (dBi)
7	9135-9382 (247)	5.936	9162-9411 (249)	5.733	9081-9319 (238)	5.809
8	9115-9335 (220)	5.576	9154-9373 (219)	5.619	9087-9314 (227)	5.543
9	9101-9288 (187)	5.347	9155-9305 (150)	5.403	9199-9334 (135)	5.486

Tab. 10. Axial Ratio Bandwidth (ARBD) and gain variation for different hc and  $\theta_c$  when hr = 1 mm.

hc (mm)	$\theta_c = 155^\circ$		$\theta_c = 160^\circ$		$\theta_c = 165^\circ$	
	ARBD (MHz)	Gain (dBi)	ARBD (MHz)	Gain (dBi)	ARBD (MHz)	Gain (dBi)
7	9130-9368 (238)	6.1	9158-9400 (242)	5.851	9074-9305 (231)	5.888
8	9113-9328 (215)	5.775	9150-9366 (216)	5.693	9085-9311 (226)	5.709
9	9096-9281 (185)	5.444	9146-9304 (158)	5.545	9088-9299 (211)	5.355

Tab. 11. Axial Ratio Bandwidth (ARBD) and gain variation for different hc and  $\theta_c$  when hr = 2 mm.

hc (mm)	$\theta_c = 155^\circ$		$\theta_c = 160^\circ$		$\theta_c = 165^\circ$	
	ARBD (MHz)	Gain (dBi)	ARBD (MHz)	Gain (dBi)	ARBD (MHz)	Gain (dBi)
7	9125-9355 (230)	6.253	9157-9391 (234)	5.999	9073-9300 (227)	5.962
8	9119-9328 (209)	5.904	9149-9359 (210)	5.730	9086-9309 (223)	5.791
9	9103-9289 (186)	5.5	9147-9305 (158)	5.610	9090-9296 (206)	5.464

Tab. 12. Axial Ratio Bandwidth (ARBD) and gain variation for different hc and  $\theta_c$  when hr = 3 mm.

hc (mm)	$\theta_c = 155^\circ$		$\theta_c = 160^\circ$		$\theta_c = 165^\circ$	
	$\phi=0^\circ$	$\phi=90^\circ$	$\phi=0^\circ$	$\phi=90^\circ$	$\phi=0^\circ$	$\phi=90^\circ$
7	H: -27° to 54° (81°)	H: -57° to 55° (112°)	H: -26° to 55° (81°)	H: -55° to 55° (110°)	H: -31° to 56° (87°)	H: -59° to 60° (119°)
	A: -28° to 43° (71°)	A: -53° to 56° (109°)	A: -24° to 47° (71°)	A: -54° to 57° (111°)	A: -59° to 34° (93°)	A: -56° to 54° (110°)
	U: 70°	U: 108°	U: 71°	U: 109°	U: 65°	U: 110°
8	H: -27° to 55° (82°)	H: -61° to 59° (120°)	H: -27° to 57° (84°)	H: -59° to 59° (118°)	H: -29° to 58° (87°)	H: -62° to 63° (125°)
	A: -55° to 44° (99°)	A: -54° to 57° (111°)	A: -53° to 50° (103°)	A: -54° to 57° (111°)	A: -56° to 38° (94°)	A: -55° to 55° (110°)
	U: 71°	U: 111°	U: 77°	U: 111°	U: 67°	U: 110°
9	H: -27° to 57° (84°)	H: -66° to 63° (129°)	H: -26° to 58° (84°)	H: -63° to 63° (84°)	H: -25° to 59° (84°)	H: -59° to 64° (123°)
	A: -54° to 40° (94°)	A: -56° to 61° (117°)	A: -55° to 49° (104°)	A: -57° to 60° (117°)	A: -56° to 36° (112°)	A: -56° to 59° (115°)
	U: 67°	U: 117°	U: 75°	U: 117°	U: 61°	U: 117°

Tab. 13. Variation of HPBW (H), ARBW (A) and USBW (U) for different hc and  $\theta_c$  when hr = 1 mm.

From the tables we observe that for all values of hr, the USBW in  $\phi = 0^\circ$  plane is maximum when  $hc = 8$  mm whereas the USBW in  $\phi = 90^\circ$  plane is maximum when  $hc = 9$  mm. The USBW in  $\phi = 0^\circ$  plane is maximum for  $\theta_c = 160^\circ$  whereas there is not much variation of USBW in  $\phi = 90^\circ$  plane with  $\theta_c$ .

Finally we summarize all the antenna configurations presented here. The U-slot loaded corner truncated patch antenna is Antenna A with the dimensions  $a = 9.4$  mm,  $i = 1.9$  mm,  $d = 4.2$  mm,  $L_x = 3.2$  mm,  $L_y = 2.6$  mm,  $g = 0.4$  mm,  $u = 3.9$  mm and  $s = 11.4$  mm. When this antenna is mounted upon a conical ground of dimensions  $rt = 5$  mm,  $hc = 8$  mm and  $\theta_c = 160^\circ$ , we term it as Antenna B.

hc (mm)	$\theta_c = 155^\circ$		$\theta_c = 160^\circ$		$\theta_c = 165^\circ$	
	$\phi=0^\circ$	$\phi=90^\circ$	$\phi=0^\circ$	$\phi=90^\circ$	$\phi=0^\circ$	$\phi=90^\circ$
7	H: -26° to 54° (80°)	H: -58° to 56° (114°)	H: -26° to 56° (84°)	H: -56° to 56° (112°)	H: -30° to 57° (87°)	H: -60° to 60° (120°)
	A: -28° to 44° (72°)	A: -54° to 56° (110°)	A: -24° to 48° (72°)	A: -54° to 56° (110°)	A: -54° to 37° (91°)	A: -57° to 55° (112°)
	U: 70°	U: 110°	U: 72°	U: 110°	U: 67°	U: 112°
8	H: -26° to 55° (81°)	H: -61° to 59° (120°)	H: -26° to 57° (83°)	H: -59° to 60° (119°)	H: -28° to 58° (86°)	H: -62° to 64° (126°)
	A: -53° to 45° (98°)	A: -55° to 58° (113°)	A: -52° to 51° (103°)	A: -55° to 57° (112°)	A: -49° to 40° (89°)	A: -56° to 56° (112°)
	U: 71°	U: 113°	U: 77°	U: 112°	U: 68°	U: 112°
9	H: -26° to 57° (83°)	H: -66° to 63° (129°)	H: -26° to 59° (85°)	H: -63° to 63° (126°)	H: -25° to 60° (85°)	H: -66° to 67° (133°)
	A: -51° to 41° (92°)	A: -56° to 61° (117°)	A: -53° to 49° (102°)	A: -57° to 59° (116°)	A: -38° to 40° (78°)	A: -55° to 57° (112°)
	U: 67°	U: 117°	U: 75°	U: 116°	U: 65°	U: 112°

Tab. 14. Variation of HPBW (H), ARBW (A) and USBW (U) for different hc and  $\theta_c$  when hr = 2 mm.

hc (mm)	$\theta_c = 155^\circ$		$\theta_c = 160^\circ$		$\theta_c = 165^\circ$	
	$\phi=0^\circ$	$\phi=90^\circ$	$\phi=0^\circ$	$\phi=90^\circ$	$\phi=0^\circ$	$\phi=90^\circ$
7	H: -25° to 54° (79°)	H: -58° to 28° (86°)	H: -25° to 56° (81°)	H: -28° to 28° (56°)	H: -30° to 57° (87°)	H: -60° to 61° (121°)
	A: -47° to 45° (92°)	A: -55° to 56° (111°)	A: -27° to 49° (76°)	A: -55° to 57° (112°)	A: -51° to 39° (90°)	A: -58° to 55° (113°)
	U: 70°	U: 83°	U: 74°	U: 56°	U: 69°	U: 113°
8	H: -25° to 55° (80°)	H: -62° to 60° (122°)	H: -26° to 57° (83°)	H: -60° to 60° (120°)	H: -28° to 59° (87°)	H: -63° to 64° (127°)
	A: -51° to 46° (97°)	A: -55° to 58° (113°)	A: -51° to 51° (102°)	A: -56° to 58° (114°)	A: -46° to 41° (87°)	A: -56° to 56° (112°)
	U: 71°	U: 113°	U: 77°	U: 114°	U: 69°	U: 112°
9	H: -26° to 57° (83°)	H: -66° to 63° (129°)	H: -25° to 59° (84°)	H: -63° to 64° (127°)	H: -25° to 61° (86°)	H: -66° to 68° (134°)
	A: -50° to 41° (91°)	A: -57° to 61° (118°)	A: -50° to 49° (99°)	A: -59° to 61° (120°)	A: -32° to 38° (70°)	A: -57° to 59° (136°)
	U: 67°	U: 118°	U: 74°	U: 120°	U: 63°	U: 116°

Tab. 15. Variation of HPBW (H), ARBW (A) and USBW (U) for different hc and  $\theta_c$  when hr = 3 mm.

Parameter	Antenna A	Antenna B	Antenna C	Antenna D
AR Bandwidth (GHz) (%)	8.871–9.098 (2.53)	8.914–9.123 (2.32)	9.162–9.360 (2.14)	9.150–9.366 (2.33)
ARBW ( $\phi = 0^\circ$ )	-81°–62° (143°)	-97°–62° (159°)	-54°–47° (101°)	-52°–51° (103°)
ARBW ( $\phi = 90^\circ$ )	-109°–67° (176°)	-67°–67° (134°)	-60°–60° (120°)	-55°–57° (112°)
HPBW ( $\phi = 0^\circ$ )	-47°–42° (89°)	-56°–58° (114°)	-29°–33° (62°)	-26°–57° (83°)
HPBW ( $\phi = 90^\circ$ )	-49°–41° (90°)	-64°–54° (118°)	-31°–32° (63°)	-59°–60° (119°)
USBW ( $\phi = 0^\circ$ )	-47°–42° (89°)	-56°–58° (114°)	-29°–33° (62°)	-26°–51° (77°)
USBW ( $\phi = 90^\circ$ )	-49°–41° (90°)	-64°–54° (118°)	-31°–32° (63°)	-55°–57° (112°)
Impedance Bandwidth (GHz) (%)	8.509–9.521 (11.2)	8.557–9.512 (10.6)	8.814–9.673 (9.29)	8.816–9.651 (9.04)
Gain (dBi)	6.495	4.995	6.900	5.693

Tab. 16. Variation of various antenna parameters for different antenna configurations.

Placing two of these antenna inside the nosecone radome specified previously is denoted as Antenna C. When a conical metallic ring of dimension  $tr = 1$  mm and  $hr = 2$  mm is placed inside the radome, we term it as Antenna D.

If we observe the ARBW of Antenna A in both the  $\phi = 0^\circ$  and  $\phi = 90^\circ$  planes, it is  $143^\circ$  and  $176^\circ$  which changes to  $159^\circ$  and  $134^\circ$  respectively for Antenna B. There is a decline in ARBW when the radome is placed as seen for Antenna C. The ARBW is not improved even after placing the conical ring as evident for Antenna D. The HPBW of Antenna A is around  $90^\circ$  in both the planes which improves by approximately  $25^\circ$  in Antenna B due to the presence of conical ground plane. But in Antenna C the HPBW drastically reduces to around  $60^\circ$  due to the radome. Placing the conical ring in Antenna D improves the HPBW by  $20^\circ$  and  $60^\circ$  in  $\phi = 0^\circ$  and  $\phi = 90^\circ$  planes respectively. The USBW performance of the antenna configurations A, B and C is same as the HPBW since the ARBW is always more than the HPBW. For Antenna D the USBW is determined by the HPBW in  $\phi = 0^\circ$  and ARBW in  $\phi = 90^\circ$  plane. The impedance bandwidth is high for all the antenna configurations. The gain of Antenna B is less than that of Antenna A as the beamwidth increases due to the conical ground. However the gain of Antenna C is more than that of Antenna B as the radome decreases the beamwidth. The gain of Antenna D decreases since the conical ring again increases the beamwidth of the antenna.

### 5. Results

Enclosing the two antenna system inside the radome and placement of the conical ring structure leads to a change in the frequency at which the minimum axial ratio is obtained by a few MHz. The dimensions of the antenna are changed such that the minimum value of the axial ratio is achieved at 9 GHz. The final antenna dimensions are

$a = 9.6$  mm,  $i = 1.7$  mm,  $d = 4.2$  mm,  $L_x = 3.4$  mm,  $L_y = 2.6$  mm,  $g = 0.4$  mm,  $u = 3.9$  mm and  $s = 11.6$  mm and the dimensions of the conical ground are  $r_t = 5$  mm,  $r_b = 8$  mm and  $h_c = 9$  mm. The dimensions of the conical ring are  $r_t = 1$  mm and  $h_r = 2$  mm. The patch antennas are fabricated on ARLON AD 250 substrate. The fabricated antenna structure is shown in Fig. 8.

The reflection coefficients of the two antenna system as obtained from simulation and measurement are shown in Fig. 9. The simulated impedance bandwidth is 526 MHz and the measured impedance bandwidth is around 564 MHz. The isolation between the two antennas is better than 20 dB for all the frequencies.

The variation of axial ratio with frequency as obtained from simulation and measurement is shown in Fig. 10. The simulated 3dB ARBD is 188 MHz (2.087%) whereas the measured 3dB ARBD is around 176 MHz (1.976%).

The simulated and measured radiation pattern of the RHCP antenna in both the  $\phi = 0^\circ$  and  $\phi = 90^\circ$  plane is shown in Fig. 11. The variation of gain with frequency as obtained from simulation and measurement is shown in Fig. 12.

The simulated HPBW in the  $\phi = 0^\circ$  and  $\phi = 90^\circ$  plane is  $86^\circ$  and  $123^\circ$  respectively. The simulated AR beamwidth

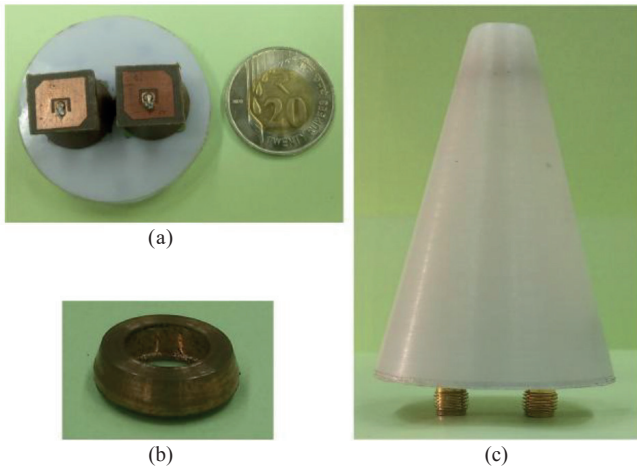


Fig. 8. Fabricated antenna structure: (a) two antenna system placed on conical ground, (b) metallic conical ring and (c) final assembly.

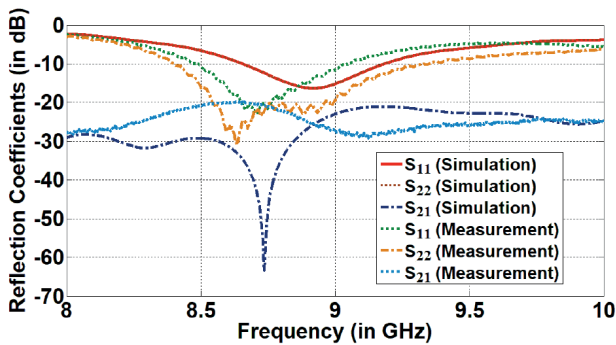


Fig. 9. Reflection coefficient of the antenna system.

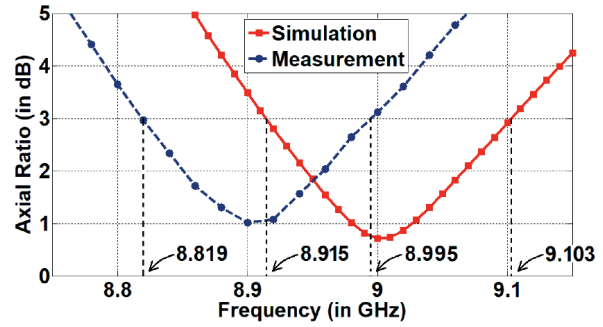


Fig. 10. Axial ratio variation with frequency.

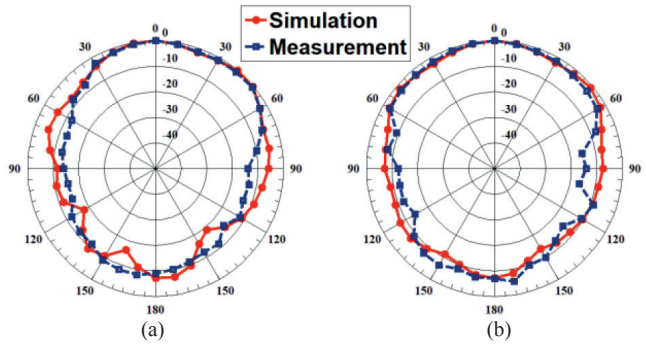


Fig. 11. Normalized radiation pattern of the antenna in (a)  $\phi = 0^\circ$  plane and (b)  $\phi = 90^\circ$  plane.

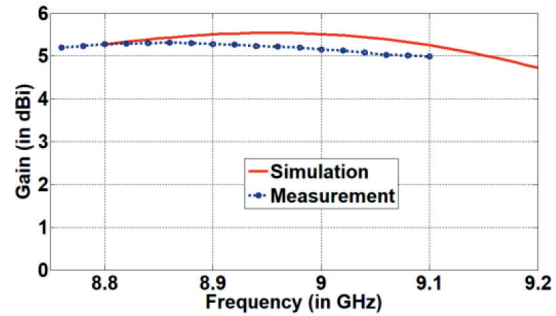


Fig. 12. Variation of gain with frequency.

in the  $\phi = 0^\circ$  and  $\phi = 90^\circ$  plane is  $74^\circ$  and  $120^\circ$  respectively. Therefore the USBW of the antenna becomes  $74^\circ$  and  $120^\circ$  in the  $\phi = 0^\circ$  and  $\phi = 90^\circ$  plane respectively. The simulated cross-polar discrimination of the antenna is around 25 dB. The simulated gain of the antenna is 5.542 dBi and the measured gain is 5.31 dBi. The simulated efficiency of the antenna is more than 90% in the frequencies of operation.

## 6. Conclusion

A U-slot loaded corner truncated microstrip patch antenna was chosen due to its ability to produce wide bandwidth CP radiation pattern. In order to improve the beamwidth of the antenna it was placed upon a conical shaped ground plane and parametric studies were carried out in order to understand the relation between the antenna parameters and the conical ground dimensions. When two such identical antennas mounted on conical ground, one

having RHCP response and another having LHCP response were placed inside a nosecone radome, a drastic reduction in the beamwidth was observed. Finally placement of a metallic conical ring structure inside the radome in the topmost part led to increase in the antenna beamwidth.

## Acknowledgments

The authors would like to thank ARDE, DRDO for giving us an opportunity to work under a sponsored project.

## References

- [1] BAHL, I. J., BHARTIA, P., STUCHLY, S. Design of microstrip antennas covered with a dielectric layer. *IEEE Transactions on Antennas and Propagation*, 1982, vol. 30, no. 2, p. 314–318. DOI: 10.1109/TAP.1982.1142766
- [2] ROUDOT, B., MOSIG, J. R., GARDIOL, F. E. Radome effects on microstrip antenna parameters. In *Proceedings of the 17th European Microwave Conference*. Rome (Italy), September 1987, p. 771–777. DOI: 10.1109/EUMA.1987.333712
- [3] LUK, K. M., TAM, W. Y. Microstrip antennas covered with dielectric materials. In *Digest on Antennas and Propagation Society International Symposium*. San Jose (CA, USA), June 1989, p. 616–619. DOI: 10.1109/APS.1989.134762
- [4] MEAGHER, C. J., SHARMA, S. K. Investigations on an aperture-coupled microstrip patch antenna with a spaced dielectric cover for enhanced gain performance. In *Proceedings of the 13th International Symposium on Antenna Technology and Applied Electromagnetics and the Canadian Radio Science Meeting*. Alberta (Canada), February 2009, p. 1–4. DOI: 10.1109/ANTEMURSI.2009.4805088
- [5] YANFEI, L., MITTRA, R., GUIZHEN, L., et al. Realization of high directivity enhancement by using an array of microstrip patch antennas (MPAs) covered by a dielectric superstrate. In *Proceedings of the Loughborough Antennas and Propagation Conference*. Loughborough (UK), November 2009, p. 493–495. DOI: 10.1109/LAPC.2009.5352503
- [6] CHEN, K. S., LIN, K. H., SU, H. L. Microstrip antenna gain enhancement by metamaterial radome with more subwavelength holes. In *Proceedings of the Asia Pacific Microwave Conference*. Singapore, December 2009, p. 790–792. DOI: 10.1109/APMC.2009.5384268
- [7] SANTOSO, S. A., HAMID, S., CHALERMWISUTKUL, S., et al. High gain resonant cavity antenna integrated with frequency selective surface radome absorber. In *Proceedings of the 13th International Congress on Artificial Materials for Novel Wave Phenomena (Metamaterials)*. Rome (Italy), September 2019, p. 366–368. DOI: 10.1109/MetaMaterials.2019.8900919
- [8] LI, Z. Y., LI, S. J., HAN, B. W., et al. Quad-band transmissive metasurface with linear to dual-circular polarization conversion simultaneously. *Advanced Theory and Simulations*, August 2021, vol. 4, no. 8. DOI: 10.1002/adts.202100117
- [9] SU, H. L., HUANG, H. C., LIN, K. H., et al. Gain-enhanced metamaterial radome for circularly-polarized antenna. In *Proceedings of the IEEE Antennas and Propagation Society International Symposium*. Toronto (Canada), July 2010, p. 1–4. DOI: 10.1109/APS.2010.5560916
- [10] RASHEED, O., JAMLOS, M. F., SOH, P. J., et al. Improvement of a circular polarized patch antenna using a split ring resonators-based radome. In *Proceedings of the International Symposium on Antennas and Propagation*. Xian (China), October 2019, p. 1–3.
- [11] KOZAKOFF, D. J. *Analysis of Radome-enclosed Antennas*. 2<sup>nd</sup> ed. London (UK): Artech House, 2010. ISBN: 978-1-59693-441-2
- [12] MENG, H., DOU, W. Multi-objective optimization of radome performance with the structure of local uniform thickness. *IEICE Electronics Express*, October 2008, vol. 5, no. 20, p. 882–887. DOI: 10.1587/elex.5.882
- [13] HSU, F., CHANG, P. R., CHAN, K. K. Optimization of two dimensional radome boresight error performance using simulated annealing technique. *IEEE Transactions on Antennas and Propagation*, September 1993, vol. 41, no. 9, p. 1195–1203. DOI: 10.1109/8.247745
- [14] XU, W., DUAN, B. Y., LI, P., et al. Multiobjective particle swarm optimization of boresight error and transmission loss for airborne radomes. *IEEE Transactions on Antennas and Propagation*, 2014, vol. 62, no. 11, p. 5880–5885. DOI: 10.1109/TAP.2014.2352361
- [15] XU, W., DUAN, B. Y., LI, P., et al. A new efficient thickness profile design method for streamlined airborne radomes. *IEEE Transactions on Antennas and Propagation*, November 2017, vol. 65, no. 11, p. 6190–6195. DOI: 10.1109/TAP.2017.2754460
- [16] NAIR, R. U., SHASHIDHARA, S., JHA, R. M. Novel inhomogeneous planar layer radome design for airborne applications. *IEEE Antennas and Wireless Propagation Letters*, 2012, vol. 11, p. 854–856. DOI: 10.1109/LAWP.2012.2210531
- [17] ZHOU, L., PEI, Y., FANG, D. Dual-band A-sandwich radome design for airborne applications. *IEEE Antennas and Wireless Propagation Letters*, 2015, vol. 15, p. 218–221. DOI: 10.1109/LAWP.2015.2438552
- [18] WANG, D. Broadband modified B sandwich as radome's layer structure. *Journal of Electronics*, October 1994, vol. 11, no. 4, p. 332–338. DOI: 10.1007/BF02778387
- [19] ILAVARASU, S., NIRANJANAPPA, A. C., SINGH, M., et al. An approach to the design of composite radome for airborne surveillance application. *International Journal of Mechanical Engineering and Technology*, 2018, vol. 9, no. 2, p. 36–48. ISSN: 0976-6340
- [20] NAIR, R. U., SUPRAVA, M., JHA, R. M. Graded dielectric inhomogeneous streamlined radome for airborne applications. *Electronics Letters*, May 2015, vol. 51, no. 11, p. 862–863. DOI: 10.1049/el.2015.0462
- [21] LIU, J., LI, L., ZUO, Y., et al. Analysis of performance degradation introduced by radome for high-precision GNSS antenna. *International Journal of Antennas and Propagation*, 2019, vol. 2019, p. 1–13. DOI: 10.1155/2019/1529656
- [22] TANG, C. L., CHIOU, J. Y., WONG, K. L. Beamwidth enhancement of a circularly polarized microstrip antenna mounted on a three-dimensional ground structure. *Microwave and Optical Technology Letters*, January 2002, vol. 32, no. 2, p. 149–153. DOI: 10.1002/mop.10116
- [23] SU, C. W., HUANG, S. K., LEE, C. H. CP microstrip antenna with wide beamwidth for GPS band application. *Electronics Letters*, September 2007, vol. 43, no. 20, p. 1062–1063. DOI: 10.1049/el:20071691
- [24] PRADHAN, S., GUPTA, B. Wideband circularly polarized microstrip antenna with enhanced beamwidth. In *Proceedings of the URSI Asia-Pacific Radio Science Conference (AP-RASC)*. New Delhi (India), March 2019, p. 1–4. DOI: 10.23919/URSIAP-RASC.2019.8738230
- [25] WWW.CSTSTUDIO.COM